Biochimica et Biophysica Acta 1848 (2015) 976–983

Contents lists available at ScienceDirect

Biochimica et Biophysica Acta

journal homepage: www.elsevier.com/locate/bbamem

A mechanistic role of Helix 8 in GPCRs: Computational modeling of the dopamine D2 receptor interaction with the GIPC1–PDZ-domain

Ozge Sensoy, Harel Weinstein *

Department of Physiology and Biophysics, Weill Medical College of Cornell University, New York, NY, USA

ARTICLE INFO

Article history:
Received 1 August 2014
Received in revised form 15 November 2014
Accepted 2 December 2014
Available online 12 January 2015

Keywords:
GPCR signaling
GPCR–PDZ interaction
Biased molecular dynamics
Steered molecular dynamics simulation
Palmitoylation and depalmitoylation
Membrane insertion GPCR–membrane interaction

ABSTRACT

Helix-8 (Hx8) is a structurally conserved amphipathic helical motif in class-A GPCRs, adjacent to the C-terminal sequence that is responsible for PDZ-domain-recognition. The Hx8 segment in the dopamine D2 receptor (D2R) constitutes the C-terminal segment and we investigate its role in the function of D2R by studying the interaction with the PDZ-containing GIPC1 using homology models based on the X-ray structures of very closely related analogs: the D3R for the D2R model, and the PDZ domain of GIPC2 for GIPC1–PDZ. The mechanism of this interaction was investigated with all-atom unbiased molecular dynamics (MD) simulations that reveal the role of the membrane in maintaining the helical fold of Hx8, and with biased MD simulations to elucidate the energy drive for the interaction with the GIPC1–PDZ. We found that it becomes more favorable energetically for Hx8 to adopt the extended conformation observed in all PDZ–ligand complexes when it moves away from the membrane, and that C-terminus palmitoylation of D2R enhanced membrane penetration by the Hx8 backbone. Depalmitoylation enables Hx8 to move out into the aqueous environment for interaction with the PDZ domain. All-atom unbiased MD simulations of the full D2R–GIPC1-PDZ complex in sphingolipid/cholesterol membranes show that the D2R carboxyl C-terminus samples the region of the conserved GFGL motif located on the carboxylate-binding loop of the GIPC1–PDZ, and the entire complex distances itself from the membrane interface. Together, these results outline a likely mechanism of Hx8 involvement in the interaction of the GPCR with PDZ-domains in the course of signaling.

1. Introduction

G-protein-coupled receptors (GPCRs) are seven-transmembrane (7-TM) domain proteins that serve as the primary site of action for signal transduction that proceeds through a network of protein–protein interactions at, and near, the cell membrane. The activation of GPCRs by extracellular signals that extracellular agents of large variety in molecular size and pharmacological characteristics [1] leads directly to association with effectors that transduce the signal into the cell. As their name indicates, these receptors associate most often with heterotrimeric G proteins for which they serve as guanine nucleotide exchange factors (GEFs) [2], which respond in turn [3] by activating a wide variety of cellular effectors including enzymes and ion channels through a variety of specialized mechanisms in what is known as the signaling cascade [4]. The termination of the signaling by the activated GPCR involves its phosphorylation by kinases in the GRK family, and binding to Arrestins. More recently, Arrestin binding itself has been shown to activate intracellular pathways in G-protein-independent signaling [5]. The time-ordered interaction of the activated GPCRs with effector proteins in the signaling cascade is regulated by the local signalosome which most often includes proteins that include PDZ domains that scaffold and direct local interactions [6] by binding to the distal C-terminal of the GPCR. PDZ-domains have been initially classified into three classes based on the amino acids that constitute the C-terminal motif of the target protein for which the PDZ domain exhibits selectivity: (i) class I domains recognize the S/T-X-ϕ motif, (ii) class II recognize ϕ-X-ϕ and (iii) class III domains recognize the D/E-X-ϕ motif, where X stands for any residue, and ϕ is a hydrophobic residue.

Elements of the complex signaling interaction network have become clearer from accumulating structural information at the molecular level, such as the breakthrough crystal structures of class A GPCRs and their complexes with G proteins [7–11]. Based on such structural information, detailed attention was accorded to the function-related conformational changes in the TM bundle of GPCRs, but less so to the amphipathic helical motif, Helix-8 (Hx8), which is located immediately after the end of the seventh transmembrane domain. Yet the conservation of such a structure in nearly all class A GPCRs suggests a specific role for this domain in GPCR signaling. Such a role is also supported by results from

Abbreviations: GPCR, G-protein-coupled receptor; Hx8, Helix-8; TM7, seven transmembrane

* Corresponding author at: Office Location: 1300 York Avenue, New York, NY 10065, USA. Tel.: +1 212 746 6358.
E-mail address: haw2002@med.cornell.edu (H. Weinstein).

http://dx.doi.org/10.1016/j.bbamem.2014.12.002

experimental studies that have indicated the possible involvement of Hx8 in various cellular processes such as G-protein coupling [12], regulation of activation [13], receptor expression [14], and internalization [15]. The likelihood of a direct contribution of this structural domain to GPCR signaling is supported by the finding — in various crystal structures [16,17] and long atomistic simulations [18] of receptors with different ligands — that Hx8 changes its positional preference. In addition, Hx8 was shown to act as a membrane-dependent conformational switch-domain, adopting a helical structure only in the presence of membrane or membrane-mimetics [19]. This reinforced the notion of the possible participation of Hx8, through dynamic changes, in the transduction of signals by the full GPCR (i.e., signal transduction by ligand binding from the extracellular region, into the cell interior). Here we address the mechanism by which this conserved juxtamembrane structural motif participates in the signaling process by identifying structural and mechanistic underpinnings of the interactions between the receptor and GPCR-interacting proteins involved in function.

A key posttranslational modification in GPCRs is the reversible palmitoylation at a conserved cysteine residue(s) located terminally to the Hx8 segment whose state depends on the activation state of the receptor [20,21]. The effect of this post-translation modification on receptor function and trafficking has been studied [20,22,23], and the dynamics of palmitoyl groups on Hx8 of Rhodopsin within an explicit membrane environment has been investigated with long atomistic molecular dynamics (MD) simulations [24]. It remains unclear, however, how this modification affects the preferred positioning of Hx8 relative to the membrane, and what its possible functional role might be in GPCR–protein interactions involving Hx8. This gap in understanding of the likely mechanisms underlying the role of the conserved Hx8 motif in the function of the GPCRs is addressed here together with the structural and dynamic properties determining modes of interaction of Hx8, in the context of the dopamine 2 receptor (D2R) where this motif constitutes the distal C-terminal segment. To this end, we have used computational modeling and simulation to (1)-examine the effects of reversible palmitoylation on the Hx8 conformation and its membrane insertion, and (2)-investigate the binding of this Hx8 to the PDZ domain of protein GIPC1 with which it is known to interact [25], as an illustrative example of interactions underlying the functional mechanisms.

The results of the computational studies presented here provide new insights into properties and mechanisms of Hx8, obtained from large-scale regular as well as steered MD simulations and metadynamics calculations. The latter two methods are well defined and widely used approaches belonging to the class of "biased MD simulations", which are designed to improve the sampling of states and conformations available to large molecular systems, as described in detail in the Methods section. The results show how the positioning of Hx8 prepares the C-terminus of D2R for its interaction with the PDZ domain of the GIPC1 protein (termed the GIPC1–PDZ-domain). Thus, we find that de-palmitoylation decreases the membrane penetration depth of the C-terminal region, and Hx8 is rendered more accessible to the PDZ-containing protein in the aqueous environment without any significant change in its conformation. The results from unbiased all-atom MD simulations, performed to test the stability of a complete molecular model of D2R–GIPC1–PDZ-domain complex, reveal that although the C-terminal segment of the D2R cannot be considered a typical PDZ ligand (because it contains a C-terminal residue that is not usually recognized by PDZ domains, cysteine), it nevertheless interacts favorably with the GIPC1–PDZ-domain and the charged carboxyl group of the terminal cysteine residue positions itself near the main-chain amine groups located on the characteristic PDZ-carboxylate binding-loop (the "GLGF loop" [26], named for the one-letter codes of the component amino acids). When this occurs, a part of the binding groove region of the PDZ-domain moves away from the membrane, together with the terminal five residues of D2R bound in the groove. In this new position, the D2R terminus is still confined within the binding groove of PDZ-domain which interacts with the membrane through TYR and ARG residues of its conserved "crac" motif that is responsible for cholesterol binding [27].

To assess quantitatively the transition of the helix region of the D2R to an extended conformation (termed h-to-e transition) that becomes suitable for the binding of Hx8 to the PDZ-domain we used (i)-steered MD simulations, and (ii)-metadynamics calculations. These allowed us to conclude, respectively, (1)-whether the distancing from the membrane of the five-residue terminal stretch of D2R bound to the PDZ domain, by PDZ-domain, as observed in regular MD simulations, helps to unravel Hx8 and eventually directs residues to the binding groove of the PDZ-domain; and (2)-to estimate the energy required to unravel the non-palmitoylated Hx8 to the extended conformation required to interact with the PDZ-domain.

2. Methods

All simulations, including the steered MD and metadynamics calculations, were carried out with the NAnoscale Molecular Dynamics (NAMD) Package [28]. Coarse-grained (CG) simulations were done with the Martini force field [29]. Atomistic simulations were performed under constant pressure with the anisotropic pressure coupling scheme, where Langevin Piston Period was set to 400 fs, and Langevin Piston Decay was set to 100 fs. Constant temperature (310 K) was maintained throughout the simulations with Langevin Dynamics. PME [30] was used to calculate long-range electrostatic contributions. All MD simulations were performed with keeping all the bonds rigid within the system, which allows an integration-step of 2 fs. Outputs were saved every 20 ps for regular MD simulations, and 2 ps for metadynamics calculations. The receptor protein, PDZ-domain, and palmitoyl groups were modeled with the all-atom CHARMM27 force field with CMAP corrections [31]. TIP3P was used to model water molecules in the system [32]. In CG simulations, an integration step of 0.04 ps was used. Long-range electrostatic and van der Waals interactions were calculated with shift function. For the latter, we used a twin-range cut-off scheme of 0.9 and 1.2 Å with neighboring list updated every 10 ps. Berendsen algorithm [33] was used to maintain constant temperature and pressure. CG coordinates were transformed to atomistic coordinates using the transformation module, which is based on restrained simulated annealing, implemented with the Martini force field. Simulations were performed in a lipid composition of 70% sphingomyelin and 30% cholesterol to mimic lipid rafts, which act as membrane micro domains for the assembly of signaling molecules. Parameters for sphingomyelin and cholesterol in the atomistic simulations were taken from [34] and [35], respectively. All the systems were neutralized at 0.15 M NaCl. We used the STRIDE algorithm [36] implemented in the NAMD package [28] for secondary structure analyses in atomistic simulations.

2.1. Coarse-grained and atomistic MD simulations in explicit membrane representation of a system composed of the TM7–Hx8 segment from D2R

The effect of reversible palmitoylation on the conformation and depth of membrane-penetration of Hx8 in this segment was evaluated from both coarse-grained and atomistic MD simulations. The simulated system is comprised of the entire TM7 (residues 254–280) together with residues 250–253 of the extracellular loop 3, and the entire amphipathic Hx8 (residues 281–293). The palmitoylated TM7–Hx8 construct was obtained by patching the palmitoyl group to the terminal cysteine residue of Hx8, and was considered in the zwitterionic form. CG simulations were conducted first, followed by backmapping the equilibrated CG structure to its atomistic coordinates to be used in subsequent atomistic MD simulations. The backbone atoms of TM7 were restrained to their initial coordinates in order to maintain the orientation adopted by TM7 within the membrane in the presence of the complete structure of the receptor. The CG simulations of (non)-palmitoylated TM7–Hx8 were performed for 4 μs effective time, and the full atomistic

simulations for 250 ns. To determine convergence the backbone insertion depth of each residue of Hx8 was monitored between successive predetermined lengths of windows over the entire trajectory. For CG simulations, we used 100 ns windows, and for atomistic simulations we used 50 ns windows. A cutoff of 0.05 Å was used as the convergence criterion between subsequent windows. The depth of insertion of the Hx8 backbone was calculated by including the nitrogen, Cα atom, and the carbonyl group (−C═O). The average insertion was determined with respect to the phosphorous atoms of the membrane lipid headgroups present within a 2 Å cut-off distance from the backbone of Hx8.

The steered molecular dynamics (SMD) simulations of the TM7–Hx8 construct were also carried out with the backbone atoms of TM7 restrained to initial coordinates, in order to maintain the orientation it had within the membrane in the presence of the other TMs of the D2R. For the constant velocity pulling, a spring constant of 1 kcal/mol × Å^2 was applied on the Cα of the P_0 residue (i.e., the most C-terminal residue of the TM7–Hx8 construct), in the negative Z direction. The results are presented for the very low pulling velocity of 0.005 Å/ps. Pulling was continued until the P_{-4} residue (i.e., the 5th residue from the C-terminus of the TM7–Hx8 construct), was exposed to water. Larger values of spring constant and pulling velocity produced unfolding of the patch without distancing it from the membrane, and were not used. Secondary structural change was recorded during the course of pulling.

2.2. Atomistic MD simulations of the D2R complex with the GIPC1–PDZ-domain in the membrane environment

In the absence of experimentally determined structures for D2R, GIPC1 and the D2R–GIPC1 complex, the structures were modeled with established protocols: 1)-For D2R we used a validated homology model that has served successfully in several studies combining MD simulations with experimental exploration [37]. The model was obtained by using as template the 3D structure of the D3R [11], a closely related GPCR that is classified under the same dopamine receptor subgroup. 2)-For the 3D structure of the GIPC1–PDZ-domain we employed homology modeling with GIPC2 as a template in view of the high sequence identity (65%) of the two proteins. Sequence alignment was done using BLAST [38] implemented in Swiss Model [39] with a criterion value of 5.04e^{-25}. The initial structure of the complex between the D2R C-terminus and the GIPC1–PDZ-domain was constructed on the basis of the information that the GIPC1–PDZ domain interacts with the C-terminus of D3R [25], which has a high sequence similarity with D2R. Based on the wealth of crystal structures of ligand–PDZ-domain complexes in PDB [40], and the information in PDZbase [41], we consider the terminal five-residue stretch of D2R, referred to as the pentapeptide ligand (see Fig. 1), in an extended conformation, as the ligand in the complex between the D2R and the GIPC1–PDZ-domain. The starting conformation of the complex was thus obtained by docking the pentapeptide ligand into the binding site of the GIPC1–PDZ-domain using as a template the crystal structure of the sixth PDZ-domain of GRIP1 in complex with the C-terminal peptide of liprin (PDB ID: 1N7F) [42]. This template was chosen because of the similarity that both the PDZ domain and the pentapeptide ligand bear to our system (including, like the C-terminus of D2R, a terminal cysteine residue). The pentapeptide ligand was docked to the binding groove of the GIPC1–PDZ-domain model using a PDZ-docking scheme based on simulated annealing, specifically the PDZ-DocScheme4 shown in [43] to reproduce experimentally obtained docking poses. In this docking protocol, the Cα atom of P_0 (the terminal residue of the pentapeptide ligand) was first tethered to its position by a 10 kcal/mol/Å^2 harmonic force, and then the pentapeptide ligand–GIPC1–PDZ-domain complex was minimized for 800 steps using adopted basis Newton–Raphson (ABNR) method. Next, the system was heated for over 600 ps using a 1-fs time step, temperature increments of 10 K, the leapfrog Verlet integrator, and a distance-dependent dielectric of 2r; outputs were saved every 1 ps. According to the PDZ-DocScheme4, the pentapeptide ligand and the PDZ-domain side chains within a 6 Å radius from the ligand were allowed to move while the rest of the PDZ-domain was frozen during the heating step, where the final temperature reached was 1000 K. Side chains of the residues of the pentapeptide ligand and of the PDZ-domain within the same cutoff were also kept flexible during the cooling step. Each snapshot obtained at the end of the cooling step was minimized for 300 ABNR steps. Optimization on each snapshot was then performed with SCWRL3.0 [44]. In the final step, energy minimization was carried out for 100 steps with the steepest descent method, and for 1500 steps with ABNR without the tether connecting the Cα of P_0. Each pose was scored by the sum of interaction energies between the PDZ-domain and the pentapeptide ligand, and the internal energy of the ligand itself, all calculated in CHARMM27 [31]. The plot of the resulting scoring energy against the root mean square deviation (RMSD) of heavy atoms of the pentapeptide ligand produced a funnel-like distribution whose bottom was dominated by structures with low RMSD and a high "energy score" (the scoring algorithm identifies the structure with the most negative energy calculated for the system to have the highest score). The structure with lowest RMSD and highest scoring energy was chosen as the initial structure in a second cycle of simulated annealing performed with the same procedure. No further decrease was registered in either energy or RMSD. The resulting complex between the pentapeptide ligand and the GIPC1–PDZ-domain was patched back onto the rest of the D2R structure using the "LINK" patch in CHARMM27 topology file [31]. An energy minimization was done to eliminate clashes between the membrane and the resulting patch before starting the all-atom MD simulations. For validation, two atomistic MD simulations were performed for 250 ns, each of them starting with a different seed. The D2R–GIPC1–PDZ system contained approximately 160,000 atoms.

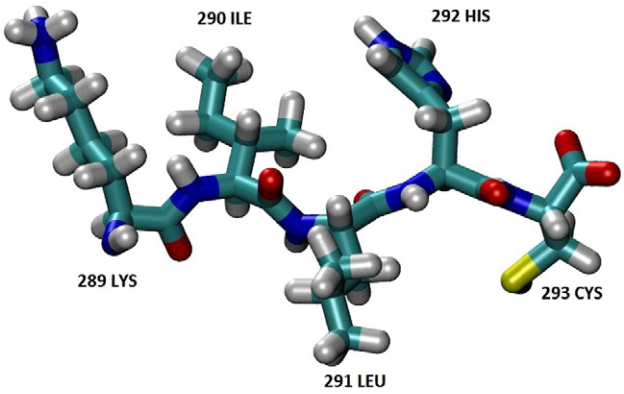

Fig. 1. The amino acid sequence corresponds to the terminal five residues of D2R (referred to as the pentapeptide ligand) is shown in Licorice representation. Amino acids are indicated by three-letter codes together with their corresponding residue numbers in the protein. Carbon, nitrogen, hydrogen, oxygen and sulfur atoms are shown in cyan, blue, white, red and yellow, respectively.

2.3. Biased MD simulations

We performed metadynamics calculations to estimate the free energy profile required to unravel (i.e., structural transition from α-helix to extended conformation) the terminal five residues of the TM7–Hx8 construct at the membrane/water interface. The free energy is calculated as a function of n pre-determined order parameters, the collective variables (CVs) that are used to construct the history-dependent bias potential defined as

$$V(R,t) = \sum_{t'<t} w_{t'} \prod_{i=1}^{n} \exp\left(-\frac{\left[s_i(R(t)) - s_i(R(t'))^2\right]}{\sigma_i^2} \right) \quad (1)$$

where s_i (R), $1 \le i \le n$ represent the CVs, t' is a multiple of deposition time τ, and $w_{t'}$ and σ_i describe, respectively, the height and width of the deposited Gaussian potentials (hills) (for a complete description of the methodology, see [45]) Here, we used a specific variant of the original metadynamics algorithm, well-tempered metadynamics, where the Gaussian height $w_{t'}$ is automatically rescaled during the simulations:

$$w_{t'} = w \exp\left(-\frac{V(R,t')}{k_B \Delta T}\right) \quad (2)$$

where ΔT is a constant with the dimension of temperature, k_B is the Boltzmann constant, and w is a constant energy representing the maximum height of Gaussian potentials. With this method, the bias potential smoothly converges to a constant value in time since the exponential factor decreases the rate of the bias-update for regions with higher bias. Finally, the free energy can be constructed as follows:

$$W(R) = -\lim_{t\to\infty} \frac{T+\Delta T}{\Delta T} V(R,t). \quad (3)$$

Metadynamics simulation was performed for the non-palmitoylated TM7–Hx8 construct in the explicit membrane representation. We used the ALPHABETA function implemented in the Plumed package [46] to describe the collective variables. These CVs were chosen to describe the helicity of the Hx8 segment (see below). The ALPHABETA function measures the approximate number of backbone dihedral angles similar to a given target angle, and is expressed as

$$s_{\alpha\beta} = 0.5 * \sum_{i=1}^{N_D} \left(1 + \cos\left(\phi_i - \phi_i^{REF}\right)\right) \quad (4)$$

where N_D corresponds to number of dihedrals considered in the calculation. In this study, $N_D = 9$ (4 residues with two dihedral angles each, and one for the C-terminal residue that was not capped). Two different ALPHABETA functions were used for the two CV sets: CV1 with target dihedral angles describing an extended conformation of the helix (-45^0, 135^0), and CV2 describing an α-helix conformation with target angle-pairs of (-60^0, -45^0). Simulation was performed for 300-ns with a bias factor of $\Delta T = 30$ T, and a deposition interval of $\tau = 0.4$ ps. The convergence was determined using smoothed bias profiles starting from the beginning up to different time intervals until the last hill was reached. Accordingly, we first took the average of the first 500 hills, and then took the average of the last 500 hills of the first 1000-hills, and so on. The convergence of the free energy difference between the two conformations is given as a function of the progress of the metadynamics simulation in Fig. A.1.

3. Results

With the computational modeling and simulation approaches described in detail in the Methods section we have (1)-examined the effects of reversible palmitoylation on the Hx8 conformation and its membrane insertion, and (2)-investigated an illustrative example of interactions underlying the functional mechanisms: the binding of this Hx8 to the PDZ domain of protein GIPC1 with which it is known to interact [25].

3.1. Effects of reversible palmitoylation on the Hx8 conformation and its membrane insertion

The comparison of MD simulation results of the TM7–Hx8 construct with and without palmitoylation showed that the palmitoyl group introduced an asymmetry in the insertion profile of residues of Hx8 in a membrane composed of 70%–30% sphingomyelin–cholesterol. Thus, the insertion depth of the five-residue-patch was increased in the presence of the palmitoyl group, whereas the rest of the residues penetrated relatively less than in the non-palmitoylated form (see Fig. 2). Cholesterol molecules present within a cutoff of 5 Å distance from the palmitoyl group, preferred to orient their hydrophobic tail parallel to it, whereas in the absence of the palmitoyl no such orientational preference was observed for the cholesterol. As this mode of palmitoyl/cholesterol interaction likely reduces the dynamic flexibility of both, it serves as an anchor helping the C-terminus of Hx8 to penetrate deeper into the membrane. Consistent with this expectation, we observed that the five-residue-patch penetrated to a lesser extent into the membrane in the absence of the post-translational modification, thus making the C-terminus of Hx8 more accessible to the aqueous environment. Interestingly, there was little difference in the conformational space explored by the Hx8 residues in the two constructs. The residues in positions P_{-2}, P_{-3}, and P_{-4} preferred to sample α-helix conformation both in the absence and in the presence of the palmitoyl group, whereas P_{-1} (penultimate residue of the five-residue-patch) preferred to sample extended conformations. We conclude that de-palmitoylation reduces the membrane insertion depth of Hx8 — identified by less negative insertion values in Fig. 2 — without much effect on its conformational preference.

3.2. The binding of this Hx8 to the PDZ domain of protein GIPC1

In all crystal structures of PDZ–ligand complexes the peptide segment bound in the binding groove of the PDZ-domain is in an extended conformation. The five-residue-patch of Hx8 will accordingly have to unfold to bind in the binding groove of the PDZ-domain. To test whether α-helical portion of Hx8 is unraveling further when such an interaction occurs, or whether the PDZ binding selects an already extended conformation of the Hx8 and stabilizes it further through the binding interaction, we utilized three separate approaches as described for each in the Methods section. In the first, we investigated the mechanism and energetics of the structural transition from α-helix to extended conformation using metadynamics simulations. In the second, we carried out steered MD simulations of the non-palmitoylated TM7–Hx8 construct in the explicit membrane representation to investigate whether distancing of the five-residue patch of Hx8 from the membrane does itself assist in the unraveling of that region. In the third, we evaluated with unbiased all-atom MD simulations the stability of the D2R–GIPC1–PDZ-domain complex formed with the D2R embedded in the membrane environment and the five-residue-patch of Hx8 docked in an extended conformation in the GIPC1–PDZ-domain.

3.2.1. The mechanism and energetics of the structural transition from α-helix to extended conformation

The mechanism and energetics of the structural transition from the α-helical conformation of Hx8 to an extended conformation was evaluated by means of well-tempered metadynamics simulation (see Methods). The notable structural evolution in this biased simulation was that when the five-residue patch of Hx8 was forced to sample the extended conformation, it moved away from the membrane towards the aqueous environment rather than aligning itself parallel to the membrane interface as seen for the α-helix conformation.

To evaluate the free energy profile of the transition from α-helix-to-extended structural transition, described by $\Delta G_{\text{extended-helix}}$, we first calculated CV1–CV2 pairs of collective variables that describe extended and α-helix conformations, from distributions sampled in the metadynamics trajectory (see Methods, Biased MD simulations), Eq. (4). For the α-helix conformation, the 4–5 and 7–8 intervals were found to be populated by CV1 and CV2, respectively. For the extended conformation, the intervals of 6–7 and 4–5 were populated by CV1, and CV2, respectively. The intervals were defined by determining the corresponding minimum and maximum CV values — calculated from Eq. (4) — sampled in both α-helix and extended conformations over the trajectory.

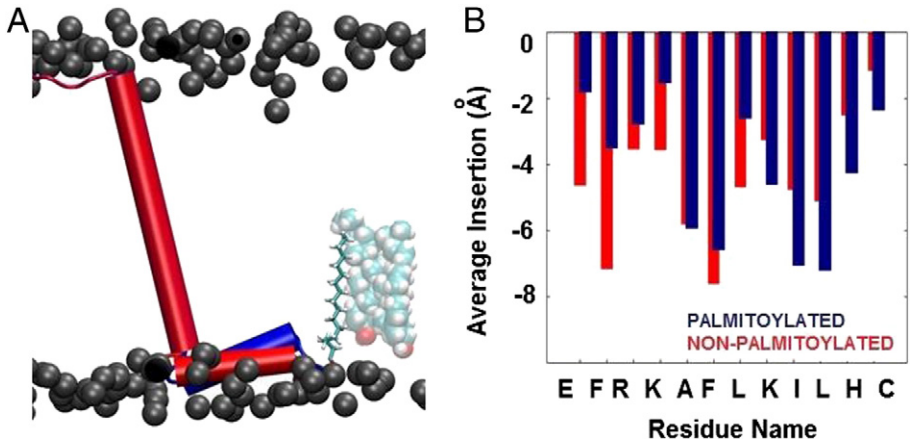

Fig. 2. Membrane insertion profiles of (non)-palmitoylated TM7–Hx8 constructs. A: Last snapshots taken from (non)-palmitoylated TM7–Hx8 simulations. TM7–Hx8 constructs are aligned with respect to their TM7s. Non-palmitoylated construct is shown in red, whereas the palmitoylated one is shown in blue with cartoon representation. The palmitoyl group is shown with Licorice representation. Nearby cholesterol molecules are shown in transparent van der Waals representation. Hydrogen atoms are shown in white, carbon atoms are shown in cyan, and oxygen atoms are shown in red color. For sake of simplicity, water molecules and lipid tails are not shown. Phosphorous atoms of the lipid molecules are shown in gray. B: Average backbone insertion values for (non)-palmitoylated TM7–Hx8 constructs. "0" corresponds to phosphorous atoms at the water-membrane interface. Negative values indicate deeper penetration to the membrane. (for details see "Coarse-grained and atomistic MD simulations in explicit membrane representation of a system composed of the TM7–Hx8 segment from D2R" of Methods section.)

The free energy surface of the structural transition constructed from the metadynamics calculation is shown in Fig. 3. In this plot, high values of CV1 (x axis) indicate that the five-residue-patch is in the extended conformation, whereas high values of CV2 (y axis) indicate that it is in α-helix conformation. The color coding shows the respective free energy expressed in kcal/mol. The most populated CV pairs sampled in the two conformations are indicated on the free energy surface by the red and black star (Fig. 3). Systematic inspection of snapshots from the metadynamics simulations confirms the direct relation between extended conformation and distancing from the membrane (as measured by the distance between the centers of mass (COM) of the peptide and the membrane patch). Finally, we calculated the amount of energy required to unravel the patch, $\Delta G_{\text{extended-helix}}$, as ~2.1 kcal/mol. We conclude that unraveling Hx8 at the membrane/water interface is not energetically favorable unless it involves its distancing from the membrane.

3.2.2. Steered MD simulations of the non-palmitoylated TM7–Hx8 construct in the explicit membrane representation

To test whether the distancing from the membrane helps to unravel the five-residue patch of Hx8 in D2R, the SMD simulation was carried out as described in Methods. The results show that pulling the target five-residue-patch out of the membrane leads to simultaneous unraveling of this segment, and directs the patch residues to the dihedral space sampled by the corresponding residues in the D2R–GIPC1–PDZ-domain complex (see Fig. 4). We conclude that distancing of the five-residue patch of Hx8 from the membrane helps the simultaneous unraveling of that region.

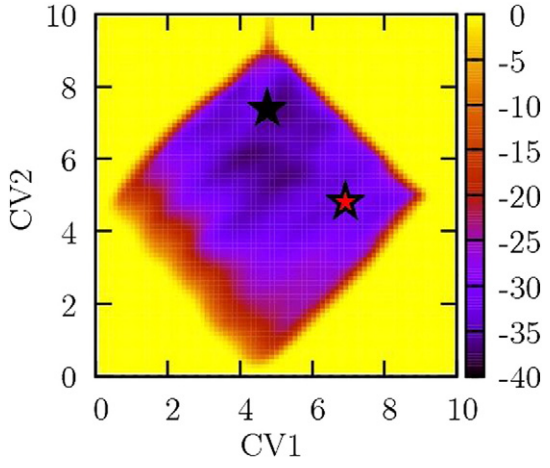

Fig. 3. Free energy surface calculated with well-tempered metadynamics. The energy scale is shown on the right with the unit in kcal/mol. Regions that correspond to α-helix (black star) and extended (red star) conformation are identified from the corresponding values of the CV1 and CV2 pairs.

3.2.3. The stability of the D2R–GIPC1–PDZ-domain complex

We used the de-palmitoylated D2R model to calculate the interaction of the C-terminus with its cytoplasmic signaling partner, the GIPC1–PDZ-domain, because we found (see above) that the palmitoylated TM7–Hx8 construct penetrates deeper into the membrane. The results show that interaction with PDZ-domain occurs with a distancing from the water/membrane interface of the five-residue-patch surrounded by the C-terminus of the α-helix (αB) and the N-terminus of the β-strand (βB) of the PDZ-domain binding groove (Fig. 5C: the five-residue patch is shown in yellow, and the corresponding part of the binding groove is shown in purple). This distancing of the bound patch from the membrane is consistent with the relation we described above between unraveling and loss of direct interaction with the membrane. In the new position, the patch is located as far as 36 Å from the membrane center, and the charged carboxyl end of the CYS residue in the P_0 position maintains its interaction with the main-chain amine groups of GLY and LEU residues of the "carboxylate loop" of the PDZ-domain (the conserved motif of R/K-X-X-X-G-L-G-F), which is the canonical mode of interaction for class I, and II ligands. The same type of interactions were seen in the crystal structure of the complex formed between the sixth PDZ-domain of GRIP1 and liprin C-terminal peptide (with PDB ID: 1N7F), where the ligand also has a terminal CYS residue [42]. It is noteworthy, however, that the N-terminus of αB in the PDZ domain, which bears the "crac" motif responsible for cholesterol binding [27,47], nevertheless maintains its interaction with the membrane through its TYR and ARG residues (see Fig. 5C: these residues are shown in Licorice representation).

As a control for the simulations of binding to the GIPC1–PDZ-domain model, we performed parallel atomistic MD simulations of the 1N7F crystal structure. The dynamics of the bound peptide in the crystal structure of the control complex, PDB ID 1N7F, were found to be very similar in all aspects to those of the five-residue patch of the D2R terminus and the binding groove of the GIPC1–PDZ-domain. Indeed the distances between the center of mass (COM) of the carboxyl group of the

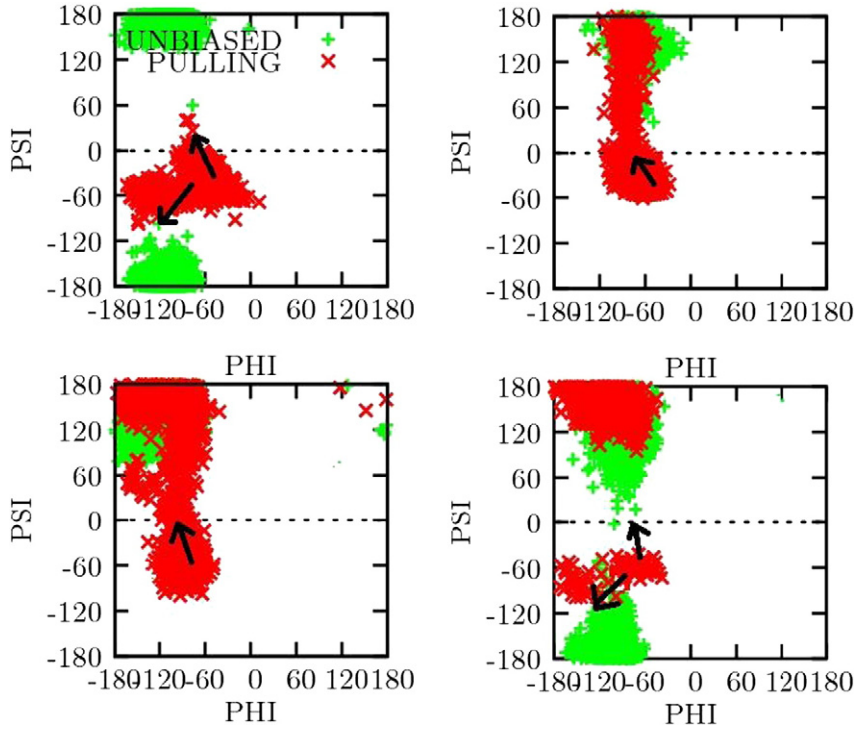

Fig. 4. Ramachandran maps showing dihedral spaces sampled by the residues of the target patch (except terminal CYS, A: P_{-1}, B: P_{-2}, C: P_{-3}, D: P_{-4}) in the pulling trajectory (red), and in regular MD simulations of the D2R–GIPC1–PDZ-domain (green). Arrows indicate the evolution of the dihedral space sampled by the target patch during the pulling.

terminal CYS residue, and the main-chain amine groups of the LEU and GLY residues of the conserved loop in the PDZ-domain, averaged over the trajectories of the compared simulations, were very similar (37 ± 1 Å for control, and 41 ± 2.1 Å in the D2R–GIPC1–PDZ complex). Moreover, the changes produced by ligand binding in the properties of the binding groove in both simulations agreed well with experimental results for the binding groove of the third PDZ-domain of PSD-95 [48]. Specifically, the aperture of the groove — defined by the distance between the Cα atoms of the middle residues of αB and βB — changed from 13 Å in the crystal structure of *apo* GIPC2–PDZ-domain to 10 Å in the bound complex. This change agrees with the experimental finding that the groove narrows upon ligand binding. We conclude that interactions between the binding groove of the PDZ-domain and the target segment is well represented by the simulations and that the corresponding energy is likely to be sufficient to overcome the energy needed to unravel this region by distancing it from the membrane. This mechanism agrees as well with the results from the Biased MD simulations in Sections 2.1, and 2.2, above.

4. Discussion

To the best of our knowledge, the insights emerging from this study offer the first mechanistic description of the dynamics and energetics of a PDZ-domain–GPCR interaction in the context of full atomistic representations of the receptor and its membrane environment. In particular, the results provide a detailed evaluation of a possible mechanistic role

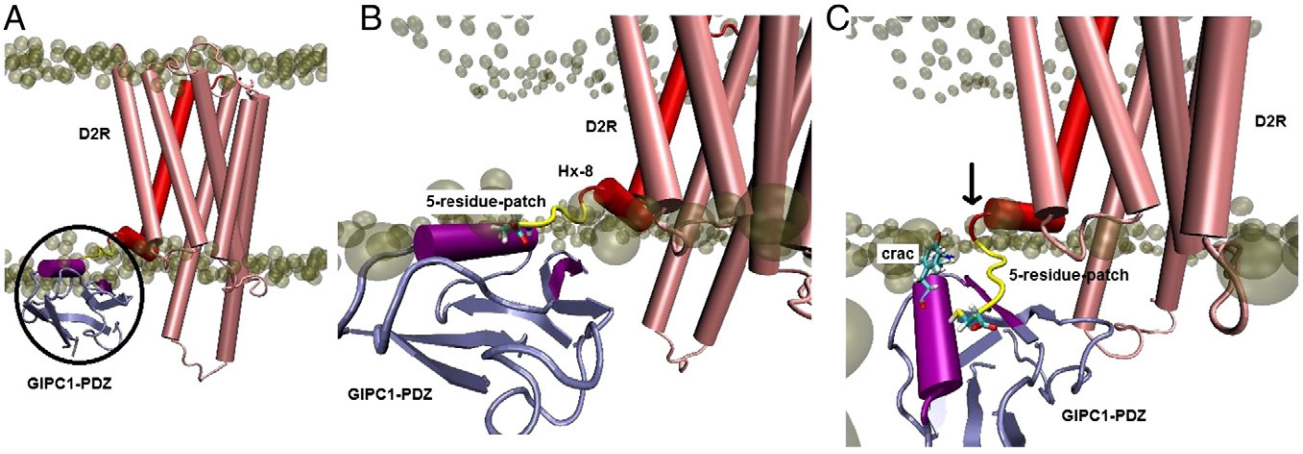

Fig. 5. A: The starting structure of the model of D2R–GIPC1–PDZ-domain complex. Transmembrane helices are shown in pink and cartoon representation except the TM7–Hx8 construct, which is shown in red. The region shown in circle is enlarged for detail in B: The five-residue patch is shown in yellow and cartoon representation. Terminal CYS residue of D2R is shown in Licorice representation, where oxygen, hydrogen, carbon, and sulfur atoms are shown in red, white, cyan and yellow, respectively. The GIPC1–PDZ-domain is shown in ice blue, except for the binding groove (composed of α-helix (αB) and β-strand (βB)), which is shown in purple. C: Final position of the binding groove of the GIPC1–PDZ-domain together with the bound five-residue-patch. The distancing of the binding groove is indicated by an arrow. Aromatic residues of the "crac" motif, (ARG and TYR residues) are also shown. Phosphate groups of the lipid membrane are shown in tan. For simplicity, the waters and lipid tails are not shown.

of Hx8 in the preparation of the C-terminus of D2R for its interaction with GIPC1–PDZ-domain. The choice of the D2R for the purpose of this investigation of the role of H-8 is based on: i) its experimentally established interaction with GIPC1–PDZ domain [25]; ii) the tractability of the problem with the relatively short C-terminal stretch comprised of only Hx8; and iii) the availability from ongoing studies in our lab of long atomistic MD simulations of the model D2R in complex with different ligands such as dopamine, sulpiride, raclopride, aripiprazole, and quinpirole. The third selection criterion is important because these simulations revealed ligand-specific structural rearrangements occurring in specific microdomains [49] of the receptor, which include the repositioning of Hx8 hypothesized to be necessary to prepare the C-terminus for its interaction with the PDZ domain. Since D2R is considered to interact with the GIPC1–PDZ-domain when bound to the agonist dopamine [25] we used long-atomistic simulations of aD2R-dopamine complex model to evaluate the mechanistic hypothesis that the part of Hx8 of D2R that interacts with the GIPC1–PDZ-domain must unravel first to the extended configuration observed in the large number of crystal structures of peptide-bound PDZ domains in all classes [41].

The simulation of the D2R–PDZ complex showed that depalmitoylation, which has been shown in many experimental studies [20,21] to occur in the context of GPCR activation, facilitates the receptor–PDZ interaction releasing Hx8 from its penetration into the membrane associated with the presence of the hydrophobic palmitoyl group. Thus, the terminal five residues in Hx8, which penetrated deeper than the others in the presence of the palmitoylation, became more exposed to the aqueous environment in its absence, suggesting that when depalmitoylation occurs under physiological conditions, a partially buried Hx8 can become accessible to proteins located in the cytoplasm that interact with GPCRs in the signaling process.

We observed that in spite of its prominent role on the depth of penetration of Hx8, depalmitoylation did not affect much the secondary structure of that region, which remained α-helical (except for the last two residues, which were in an extended conformation). Given the commonly extended structure of peptide ligands bound in the groove of PDZ domains in all crystal structures of such complexes [40,41] these results suggested that another element of the mechanism is required to unravel Hx8 for its interaction with PDZ-domain. By means of biased simulations (metadynamics and SMD) we showed (1)-that the distancing of Hx8 from the membrane is coupled to its unraveling propensity, which is in agreement with experimental findings that Hx8 loses helix conformation in the absence of the membrane [19], and (2)-that the energy required for the transition from α-helix to extended conformation, of the residue patch involved in PDZ domain binding, was ~3.5 kT. That unwinding the helical region for interaction with the PDZ domain requires a relatively low energy is likely due to the fact that the terminal two residues prefer to be in extended conformation even in the presence of the palmitoyl group, and the interaction with the PDZ-domain can guide the unraveling of Hx8 for complex formation. However, it is important to stress that the energy calculated for the TM7/Hx8 construct does not include contributions from any structural rearrangements of the TM bundle or the adjacent loops. However, detailed analyses of the trajectories revealed that although residues from intracellular loop 1 can make some contacts with Hx8, these are transient and their contribution to the energetics are likely to be very small.

The results from all-atom unbiased MD simulations of the D2R–GIPC1–PDZ-domain complex showed that the conformational extended five-residue segments of Hx8 were capable of establishing canonical interactions with the PDZ-domain, although the sequence is not typical for a PDZ ligand (see [41]) because the terminal residue is a cysteine. We found that carboxy terminus of the CYS residue interacted closely with the backbone amine groups of residues located on the conserved binding loop of PDZ-domain, which is one of the well-known canonical interactions in ligand–PDZ-domain complexes. As this complex formed, the bound segment of Hx8 together with part of the binding groove of the PDZ-domain distanced themselves from the membrane surface. The novel mechanistic insights from this study thus encompass both the role of Hx8 in establishing a functionally important interaction of the GPCR in an activated state model, and the binding of a non-typical ligand to a cognate PDZ-domain in the context of the atomistically explicit representation of the receptor and the membrane in which it is embedded.

Supplementary data to this article can be found online at http://dx.doi.org/10.1016/j.bbamem.2014.12.002.

Acknowledgements

The authors gratefully acknowledge support from the National Institute of Health grants P01DA012923, R01 MH054137, and R01 DA015170, and from TUBITAK-1059B191200320 (to O.S.), as well as the computational resource of the Institute for Computational Biomedicine at Weill Cornell Medical College. This work used the Extreme Science and Engineering Discovery Environment (XSEDE), which is supported by National Science Foundation grant number OCI-1053575 with allocations TG-MCB1130085 and TG-MCB130011 (to O.S.) on the Stampede Supercomputer system at the Texas Advanced Computing Center. The authors also acknowledge gratefully the computational resources at the National Energy Research Scientific Computing Center (NERSC), supported by the Office of Science of the U.S. Department of Energy under Contract No. DE-AC02-05CH11231.

References

[1] Brian Kobilka, G-protein-coupled receptor structure and activation, BBA-Biomembr. 1768 (2007) 794–807.
[2] J.L. Bos, H. Rehmann, A. Wittinghofer, GEFs and GAPs: critical elements in the control of small G proteins, Cell 129 (2007) 865–877.
[3] M. Rodbell, The role of hormone receptors and GTP-regulatory proteins in membrane transduction, Nature 284 (1980) 17–22.
[4] L. Rensing, Periodic geophysical and biological signals as Zeitgeber and exogenous inducers in animal organisms, Int. J. Biometeorol. 16 (1972) 113–125.
[5] Robert Lefkowitz, Sudha K. Shenoy, Transduction of receptor signals by β-arrestins, Science 308 (2005) 512–517.
[6] Randy A. Hall, Robert J. Lefkowitz, Regulation of G protein-coupled receptor signaling by scaffold proteins, Circ. Res. 91 (2002) 672–680.
[7] A. Warne, et al., Structure of a beta1-adrenergic G-protein-coupled receptor, Nature 454 (2008) 486–491.
[8] S.G.F. Rasmussen, et al., Crystal structure of the β2 adrenergic receptor–Gs protein complex, Nature 477 (2011) 549–555.
[9] T. Warne, P.C. Edwards, A.G. Leslie, C.G. Tate, Crystal structures of a stabilized β1-adrenoceptor bound to the biased agonists bucindolol and carvedilol, Structure 20 (2012) 841–849.
[10] T. Okada, M. Sugihara, A.N. Bondar, M. Elstner, P. Entel, V. Buss, The retinal conformation and its environment in rhodopsin in light of a new 2.2 Å crystal structure, J. Mol. Biol. 342 (2004) 571–583.
[11] E.Y.T. Chien, W. Liu, G.W. Han, V. Katritch, Q. Zhao, V. Cherezov, R.C. Stevens, Structure of the human dopamine D3 receptor in complex with a D2/D3 selective antagonist, Science 330 (2010) 1091–1095.
[12] O.P. Ernst, et al., Mutation of the fourth cytoplasmic loop of rhodopsin affects binding of transducin and peptides derived from the carboxyl-terminal sequences of transducin α and γ subunits, J. Biol. Chem. 275 (2000) 1937–1943.
[13] N.M. Delos Santos, L.A. Gardner, S.W. White, S.W. Bahouth, Characterization of the residues in helix 8 of the human beta1-adrenergic receptor that are involved in coupling the receptor to G-proteins, J. Biol. Chem. 281 (2006) 12896–12907.
[14] M. Tetsuka, Y. Saito, K. Imai, H. Doi, K. Maruyam, The basic residues in the membrane-proximal C-terminal tail of the rat melanin-concentrating hormone receptor 1 are required for receptor function, Endocrinology 145 (2004) 3712–3723.
[15] Y. Aratake, et al., Helix-8 of leukotriene B4 receptor 1 inhibits ligand induced internalization, FASEB J. 0892–6638 (2012) 4069–4078.
[16] K. Palczewski, et al., Crystal structure of rhodopsin: a G protein-coupled receptor, Science 289 (2000) 739–745.
[17] P. Scheerer, et al., Crystal structure of opsin in its G-protein-interacting conformation, Nature 455 (2008) 497–502.
[18] J. Shan, G. Khelashvili, S. Mondal, E.L. Mehler, H. Weinstein, Ligand-dependent conformations and dynamics of the serotonin 5-HT2A receptor determine its activation and membrane-driven oligomerization properties, PloS Comp. Biol. 8 (2012) e1002473.
[19] A.G. Krishna, S.T. Menon, T.J. Terry, T.P. Sakmar, Evidence that helix 8 of rhodopsin acts as a membrane-dependent conformational switch, Biochemistry 41 (2002) 8298–8309.
[20] J.E. Smotrys, M.E. Linder, Palmitoylation of intracellular signaling proteins: regulation and function, Annu. Rev. Biochem. 73 (2004) 559–587.

[21] T.P. Loisel, et al., Activation of the β2-adrenergic receptor–Gαs complex leads to rapid depalmitoylation and inhibition of repalmitoylation of both the receptor and Gαs, J. Biol. Chem. 274 (1999) 31014–31019.
[22] M.N. Adams, M.E. Christensen, Y. He, N.J. Waterhouse, J.D. Hooper, The role of palmitoylation in signalling, cellular trafficking and plasma membrane localization of protease-activated receptor-2, Plos ONE 6 (2011) e28018.
[23] C. Blanpain, et al., Palmitoylation of CCR5 is critical for receptor trafficking and efficient activation of intracellular signaling pathways, J. Biol. Chem. 276 (2011) 23794–23804.
[24] B.E.S. Olausson, et al., Molecular dynamics simulations reveal specific interactions of post-translational palmitoyl modifications with rhodopsin in membrane, J. Am. Chem. Soc. 134 (2012) 4324–4331.
[25] F. Jeanneteau, J. Diaz, P. Sokoloff, N. Griffon, Interactions of GIPC with dopamine D2, D3 but not D4 receptors define a novel mode of regulation of G protein-coupled receptors, Mol. Biol. Cell 15 (2004) 696–705.
[26] M.B. Kennedy, Origin of PDZ (DHR, GLGF) domains, Trends Biochem. Sci. 20 (1995) 350.
[27] M. Jafurullah, S. Tiwari, A. Chattopadhyay, Identification of cholesterol recognition amino acid consensus (CRAC) motif in G-protein coupled receptors, Biochem. Biophys. Res. Commun. 404 (2011) 569–573.
[28] J.C. Phillips, R. Braun, W. Wang, J. Gumbart, E. Tajkhorshid, et al., Scalable molecular dynamics with NAMD, J. Comput. Chem. 26 (2005) 1781–1802.
[29] S.J. Marrink, H.J. Risselada, S. Yefimov, D.P. Tieleman, A.D.J. de Vries, The Martini force field: coarse grained model for biomolecular simulations, J. Phys. Chem. B 111 (2007) 7812–7824.
[30] U. Essmann, L. Perera, M.L. Berkowitz, T. Darden, H. Lee, et al., A smooth particle mesh Ewald method, J. Chem. Phys. 103 (1995) 8577–8593.
[31] A.D. MacKerell, M. Feig, C. III, Brooks, extending the treatment of backbone energetics in protein force fields: limitations of gas-phase quantum mechanics in reproducing protein conformational distributions in molecular dynamics simulations, J. Comput. Chem. 25 (2004) 1400–1415.
[32] P. Mark, L. Nilsson, Structure and dynamics of the TIP3P, SPC, and SPC/E water models at 298 K, J. Phys. Chem. A 105 (2001) 9954–9960.
[33] H.J.C. Berendsen, J.P.M. Postma, W.F. van Gunsteren, A. Dinola, J.R. Haak, Molecular dynamics with coupling to an external bath, J. Chem. Phys. 81 (1984) 3684–3690.
[34] M.T. Hyvonen, P.T.J. Kovanen, Molecular dynamics simulation of sphingomyelin bilayer, J. Phys. Chem. B 107 (2003) 9102–9108.
[35] J.B. Lim, B. Rogaski, J.B. Klauda, Update of the cholesterol force field parameters in CHARMM, J. Phys. Chem. B 116 (2012) 203–210.
[36] M. Heinig, D. Frishman, STRIDE: a web server for secondary structure assignment from known atomic coordinates of proteins, Nucleic Acids Res. 32 (2004) W500–W502.
[37] L. Shi, J. Javitch, The second extracellular loop of the dopamine D2 receptor lines the binding-site crevice, PNAS 101 (2004) 440–445.
[38] S.F. Altschul, W. Gish, W. Miller, E.W. Myers, D.J. Lipman, Basic local alignment search tool, J. Mol. Biol. 215 (1990) 403–410.
[39] M. Biasini, et al., SWISS-MODEL: modelling protein tertiary and quaternary structure using evolutionary information, Nucleic Acids Res. 1 (2014).
[40] F.C. Bernstein, T.F. Koetzle, G.J. Williams, E.E. Meyer Jr., M.D. Brice, J.R. Rodgers, O. Kennard, T. Shimanouchi, M. Tasumi, The Protein Data Bank: a computer-based archival file for macromolecular structures, J. Mol. Biol. 112 (1977) 535–542.
[41] T. Beuming, L. Skrabanek, M.Y. Niv, P. Mukherjee, H. Weinstein, PDZBase: a protein–protein interaction database for PDZ-domains, Bioinformatics 21 (2005) 827–828.
[42] Y.J. Im, S.H. Park, S.H. Rho, J.H. Lee, G.B. Kang, M. Sheng, E. Kim, S.H. Eom, Crystal structure of GRIP1 PDZ6–peptide complex reveals the structural basis for class II PDZ target recognition and PDZ domain-mediated multimerization, J. Biol.Chem. 278 (2003) 8501–8507.
[43] M. Niv, H. Weinstein, A flexible docking procedure for the exploration of peptide binding selectivity to known structures and homology models of PDZ domains, J. Am. Chem. Soc. 127 (2005) 14072–14079.
[44] G. Krivov, M.V. Shapovalov, R.L. Dunbrack Jr., Improved prediction of protein side-chain conformations with SCWRL4, Proteins 77 (2009) 778–795.
[45] A. Barducci, G. Bussi, M. Parrinello, Well-tempered metadynamics: a smoothly converging and tunable free-energy method, Phys. Rev. Lett. 100 (2008) 020603.
[46] D. Bonomi, et al., PLUMED: a portable plugin for free-energy calculations with molecular dynamics, Comput. Phys. Commun. 180 (2009) 1961–1972.
[47] M.A. Hanson, V. Cherezov, C.B. Roth, M.T. Griffith, V.-P. Jaakola, E.Y.T. Chien, J. Velasquez, P. Kuhn, R.C. Stevens, A specific cholesterol binding site is established by the 2.8 A structure of the human beta2-adrenergic receptor, Structure 16 (2008) 897–905.
[48] S. Steiner, A. Caflisch, Peptide binding to the PDZ3 domain by conformational selection, Proteins 80 (2012) 2562–2572.
[49] I. Visiers, B.J. Ebersole, S. Dracheva, J. Ballesteros, S.C. Sealfon, H. Weinstein, Structural motifs as functional microdomains in G-protein-coupled receptors: energetic considerations in the mechanism of activation of the serotonin 5-HT2A receptor by disruption of the ionic lock of the arginine cage, Int. J. Quantum Chem. 88 (2002) 65–75.